Parameter optimal determination for canny edge detection

X M Zhao*, W X Wang and **L P Wang**
School of Information Engineering, Chang'an University, Xi'an, China

Abstract: The Canny edge detection algorithm contains a number of adjustable parameters, which can affect the computation time and effectiveness of the algorithm. To overcome the shortages, this paper proposes a new way to determine the adjustable parameters and constructs a modified Canny edge detection algorithm. In the algorithm, an image is firstly smoothed by an adaptive filter that is selected based on the properties of the image, instead of a fixed sized Gaussian filter, and then, the high and low thresholds for the gradient magnitude image are determined based on maximum cross-entropy between inter-classes and Bayesian judgment theory, without any manual operation; finally, if it needs, the object closing procedure is carried out. To test and evaluate the algorithm, a number of different images are tested and analysed, and the test results are discussed. The experiments show that the studied algorithm can achieve the better edge detection results in most of the cases, and it is also useful for object boundary closing as a pre-segmentation step.

Keywords: Bayesian, adaptive, cross-entropy, boundary closing, Canny, edge detection

1 INTRODUCTION

Since the Canny edge detection algorithm was published in 1986, the detector (including its variations) is still a state-of-the-art edge detector.[1] In last 20 years, many researchers in the world studied and are studying on Canny algorithm.

Zhu and Zhang[2] applied Otsu algorithm into Canny algorithm, which improved handling speed and parameter selection; furthermore, they then did post-process by using mathematical morphology. Their algorithm can precisely extract closed edges of fabric humid part. To overcome drawback of image processing by Gaussian filtering that might lead to the unsatisfactory edge location of the corner roundness in the traditional Canny algorithm, Shao *et al.*[3] modified Canny algorithm by replacing the Gaussian convolution with anisotropic Gaussian filtering. For reducing the defects of the traditional Canny algorithm that did not considered the neighbourhood information of a detecting pixel and therefore led to some mistakes in a complex region for the incomplete information provided by horizontal and vertical adjacent pixels, Wang *et al.*[4] presented the algorithm based on a directional filter, which used the neighbourhood information well, and carried out the multi-direction analyses on images. Kaur *et al.*[5] combined Canny algorithm and wavelet transform, in which the image smoothing and the edge detection are combined into a single step and thus wavelet-based techniques are computationally more efficient. Bao *et al.*[6] developed a scale multiplication-based scheme to improve the performance of the traditional Canny edge detector. Taking the advantage of similarities in the filter's responses at adjacent scales, the new scheme multiplies the responses to enhance edge structures while diluting noise and to detect the edges as the local maxima in the scale products. Li *et al.*[7] suggested the algorithm which can adaptively determine the two thresholds based on the gradient histogram and the minimum interclass variance; the algorithm self-adaptively calculated the two thresholds

The MS was accepted for publication on 22 October 2010.
* *Corresponding author: Xiangmo Zhao, School of Information Engineering, Chang'an University, Xi'an, China; email: xmzhao@chd.edu.cn*

 IMAG mp27 © RPS 2011 DOI: 10.1179/136821910X12867873897517

for different images without the necessity to set up any parameter artificially, and a fuzzy algorithm was adopted to choose edge pixels. He *et al.*[8] did the work on the gradient computation and the determination of edge points, in which the method performs Gaussian filtering to suppress image noise and computes gradients on the hexagonal structure. The pixel edge strengths on the square structure are then estimated before Canny edge detector is applied to determine the final edge map. Ding and Goshtasby *et al.*[9] replaced Gaussian filter with anisotropic diffusion equations, and the image enhancement was carried out after diffusion. Lv *et al.*[10] improved Canny algorithm, and this algorithm was used instead of the double-threshold one, which detected and connected edges in accordance to the difference of the gradient directions between edges and noise. To protect efficiently the details of all low-contrast edges with the noise suppressed simultaneously, Li *et al.*[11] modified the kernel function of the above edge detector according to the noise properties, and the pre-processing is also performed well. Rockett and Zhang[12] investigated the operating point of Canny edge detector, which minimised Bayesian risk of misclassification. By considering each of the sequential stages that constitute Canny algorithm, they concluded that the linear filtering stage of Canny, without post-processing, performed poorly by any standard in pattern recognition and achieved error rates that were almost indistinguishable from a priori classification. Chang *et al.*[13] modified Canny edge detector to detect retinal blood vessels, especially for small vessels. The detector was designed as a local dynamic hysteresis thresholding value generator based on Canny edge detector. It adapted the knowledge of major vessel locations to define a small neighbourhood and generate local hysteresis threshold values. The algorithm was used to detect meaningful edges, especially for the edges of small blood vessels that might be missing when using Canny edge detector alone.

All the above algorithms were studied based on Canny algorithm for either speeding up processing or/and localising edges accurately. The different algorithms have different advantages for different types of images. No one can fit all types of images. In order to detect edges accurately, based on Canny edge detector, this paper replaces Gaussian filter with an adaptive filter to smooth an image, then applies linear transformation for enhancing decreasing edges, and finally, obtains high–low threshold values according to the concept of the maximum cross-entropy between classes and Bayesian judgment theory. Experiments show that the studied algorithm can take the better edge detection results.

2 ADJUSTABLE PARAMETERS AFFECTING CANNY EDGE DETECTION

The Canny algorithm contains a number of adjustable parameters, which can affect the computation time and effectiveness of the algorithm.

For the size of the Gaussian filter, the smoothing filter used in the first stage directly affects the results of the Canny algorithm. There are two questions when smoothing an image using Gaussian filter:[14,15]

> The smoothness and the approximation are a pair of contradictions. There are two definitions and one proposition in the smoothness.
> **Definition 1:** function smoothness degree: function $g(x)$ is p-order smoothness if $g(x)$ is of p-order derivative.
> **Definition 2:** approximation degree of the function: function $g(x)$ is approximation of function $f(x)$.
> **Proposition:** assumed that $g(x)=f(x)\theta(x)$, and $\theta(x)$ is p-order smoothness function, it has:
>
> $$D=\int_{-\infty}^{+\infty}[g(x)-f(x)]^2\mathrm{d}x \tag{1}$$
>
> where D increases as p increases.
> This proposition shows that the more smoothness the smoothed image, the worse the approximation contrast to the original image. Anyhow, there is over-smoothing in Canny algorithm which smoothes an image using Gaussian filter.
> The purpose for smoothing an image is to improve SNR and decrease noise interference. Edge pixels are smoothed out as high frequency when image smoothing by using Gaussian filter, and some edge points are changed into slowly-varying edges, in which those points are condensed in the image histogram, and the points will be lost with non-maxima suppression.

In addition to the filter size for image smoothing, there are two thresholds applied in edge tracking on the gradient magnitude image. The use of the two thresholds with hysteresis allows more flexibility than in a single-threshold approach, but general problems

of thresholding approaches still apply. A threshold set too high can miss important information. On the other hand, a threshold set too low will falsely identify irrelevant information (such as noise) as important. It is difficult to give a generic threshold that works well on all images.

Making the assumption that important edges should be along continuous curves in the image allows one to follow a faint section of a given line/curve and to discard a few noisy pixels that do not constitute a line/curve but have produced large gradients. Therefore, it starts by applying a high threshold. This marks out the edges one can be fairly sure are genuine. Starting from these, using the directional information derived earlier, the edges can be traced through the image. While tracing an edge, one applies the lower threshold, allowing to trace faint sections of edges as long as one find a starting point.

Through the above analysis, one can see that the starting points of the edge detecting in a gradient image are controlled by a high threshold, and the lower the high threshold, the more the information to be reserved, and the more precise the target edges, the more spurious edges; with increasing threshold, it can suppress spurious edges effectively, but might lose the edge information. However, it is often found that a low threshold can control the characteristics of the ending edge points in edge detecting after the points above a higher threshold are founded. The smaller the low threshold, the more edge information preserved, and the more successive the edge detection; with decreasing threshold, the visual characteristics of the target edges will be less and the edge will be broken.

Based on the above analyses, in general, there are four factors affecting Canny edge detection:

1. Impact of gradient amplitude: Canny algorithm give well localisation, which calculates gradient amplitudes using finite-difference mean in a 2×2 neighbour region, but it is sensitive to noise and easily to detecting spurious edges, and loses some details of real edges.
2. Impact of non-maxima suppression: because of considering only 2 pixels, when enhancing and thinning roof edges, it will be sensitive to the noise interference and might lose some edge points that are non-continuous edges.
3. Impact of filter: the larger the filter variance σ, the smaller number of the detected edge points. Gaussian filter is a low-pass filter, but the larger the σ, the more narrow the band, and as it is useful for suppressing noise for higher frequencies, it can avoid detecting the spurious edge points. However, some edge points are missed because edge signals are smoothed. In Canny edge detection algorithm, σ is artificially set up, and different values of σ have different large effects for edge detecting; therefore, the filter coefficients are determined difficultly by considering both smoothing noise and protecting edge information.
4. Impacts of high and low thresholds: the number of edge points is determined by the choice of high and low thresholds. Naturally, the lower threshold gives more edge points, which produces more noise and affects the result of edge detecting. The idea situation of fixing the discontinuous contours in Canny algorithm is to segment an image using the fixed high and low thresholds, which is unable to consider local feature information. On the one hand, it is unable to eliminate the effects of local noise; on the other hand, it will loose local edges caused by grey value changing slowly, and lead to target contour edge discontinuous. In addition, the image edge feature information is not used to fix the parameters of high and low thresholds in Canny algorithm, while they need to be selected by an operator; therefore, Canny algorithm is not adaptive.

Based on the above analyses and discussion, a modified Canny algorithm is studied in the following to overcome the shortages.

3 DETERMINATION OF ADAPTIVE SMOOTHING FILTER AND DOUBLE-THRESHOLDS

The pixels polluted by noise make the large variances of the neighbour regions in an image. According to an image correlation rule, the pixel that cannot be polluted by noise must be correlated with statistical properties of its neighbouring region, and in the image, its grey value should be closed to its neighbouring region value, unless the singularity represents the occurrence, if it is a useful information point rather than a small probability event unexpectedly. Edge-preserving filter is to smooth an image based on the above mentioned principle. The

convolution template is shown in Fig. 1; it takes account of the effects of the different directions for its centre pixel. It is usual that the image grey-scale dynamic range will be narrower after image smoothing and some edges becoming gentler. The edge amplitudes become smaller after an image derivation operator is performed, which leads to lost edges in the double-edge detections. To change this situation, after image smoothing, a linear transformation for the image is applied. To enhance image edge contrast, image dynamic transform range is increased.

There is a growing interest in formulating vision problems in terms of Bayesian inference and, in particular, the maximum a posteriori estimator. In this study, Bayesian and cross-entropy theories are used for the determination of thresholds on a gradient magnitude image.

Cross-entropy is a measure of information difference of two probability distributions: $P=\{p_1, p_2, \ldots, p_N\}$ and $Q=\{q_1, q_2, \ldots, q_N\}$, and its definition is as follows:[16]

$$D(P,Q)=\sum_{i=1}^{N} p_i \ln\left(\frac{p_i}{q_i}\right) \tag{2}$$

Its symmetric form is called symmetric cross-entropy and the definition can be described as:

$$D(P:Q)=\sum_{i=1}^{N} p_i \ln\frac{p_i}{q_i}+\sum_{i=1}^{N} q_i \ln\frac{q_i}{p_i} \tag{3}$$

Threshold selection is often based on the principle of suitable optimization in a thresholding algorithm. Generally considering, the objects and background in an image should have a large difference as possible. An image is divided into two classes: objects (o) and background (b), and an image is supposed to have two normal distributions, in which the parameters can be obtained from the histogram of an original image:

$$p(g/i)=\frac{1}{(2\pi)^{1/2}\sigma_i}\exp\left[-\frac{g-\mu_i(t)^2}{2\sigma_i^2(t)}\right](i=\mathrm{o},\mathrm{b}) \tag{4}$$

Variances in the both categories are estimated as follows:

$$\sigma_o^2(t)=\frac{1}{P_o}\sum_{g=0}^{t} h(g)[g-\mu_o(t)]^2 \tag{5}$$

$$\sigma_b^2(t)=\frac{1}{P_b}\sum_{g=t+1}^{L} h(g)[g-\mu_b(t)]^2 \tag{6}$$

where the priori probability of object class is

$$P_o=\sum_{g=0}^{t} h(g),$$

the priori probability of background class is

$$P_b=\sum_{g=t+1}^{L} h(g),$$

so their means within clusters are

$$u_o(t)=\frac{1}{P_o}\sum_{g=0}^{t} gh(g) \text{ and}$$

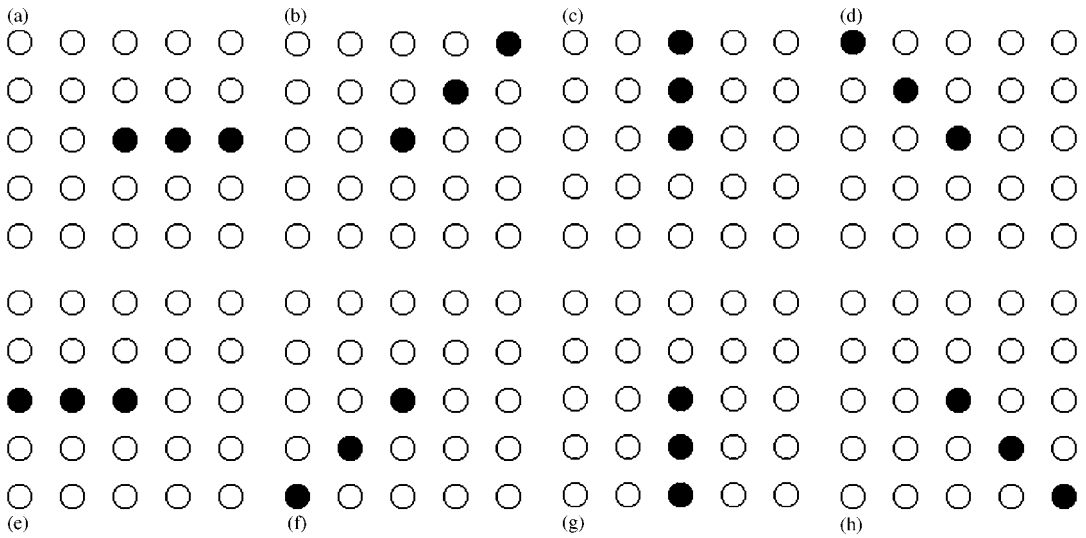

1 Adaptive filter template: (a) 0°; (b) 45°; (d) 90°; (d) 135°; (e) 180°; (f) 225°; (g) 270°; (h) 315°

a b c d

2 Experimental results of Lena image: (a) original Lena image; (b) result of Canny; (c) result of reference;[17] (d) result of the new algorithm in this paper

$$u_b(t)=\frac{1}{P_b}\sum_{g=t+1}^{L} gh(g)$$

respectively, where t is the threshold, g is the grey value and L is the grey upper bound. Then the posterior probability is obtained by using Bayesian probability formula:

$$p(i/g)=P_i p(g/i)/\sum_{i=o,b} P_i p(g/i) \tag{7}$$

The difference between the objects and the background in an image is measured using cross-entropy, combined with Bayesian judgment theory; the difference might be represented by a cross-entropy average value for every pixel in the original image P. For the object and background regions with posterior probability $p(o|s)$ and $p(b|s)$, the optimal threshold via maximum posterior probability of pixels in the different regions is obtained. Inter-class cross-entropy based on posterior probability of single pixel is

$$D(o:b;s)=\frac{1}{3}[1+p(o|s)]\ln\left[\frac{1+p(o|s)}{1+p(o|s)}\right]+\frac{1}{3}[1+p(o|s)]\ln\left[\frac{1+p(o|s)}{1+p(o|s)}\right] \tag{8}$$

The difference between classes is:

$$D(o:b)=\sum_{s\in o}\frac{p(s)}{P_o}D(o:b;s)+\sum_{s\in b}\frac{p(s)}{P_b}D(o:b;s) \tag{9}$$

Replacing the pixel grey scale s with the grey value g for simplifying the calculation is replacing a probability distribution with a grey-level histogram. Equation (9) can be re-written as:

$$D(o:b;g)=\sum_{g=0}^{T}\frac{h(g)}{P_o}D(o:b;g)+\sum_{g=T+1}^{L}\frac{h(g)}{P_b}D(o:b;g) \tag{10}$$

where L is the grey value for upper bound, and T is the grey value threshold.

To obtain the optimal threshold T^* based on maximum cross-entropy between classes, it can be carried out through a searching operation:

$$D(o:b;T^*)=\max_{T} D(o:b;T) \tag{11}$$

4 ALGORITHM DESCRIPTION

The modified algorithm firstly smoothes an image by using an adaptive filter, then pre-segments the image

a b c d

3 Experimental results for Pepper image: (a) original image; (b) result of traditional Canny; (c) result of reference;[17] (d) result of the new algorithm in this paper

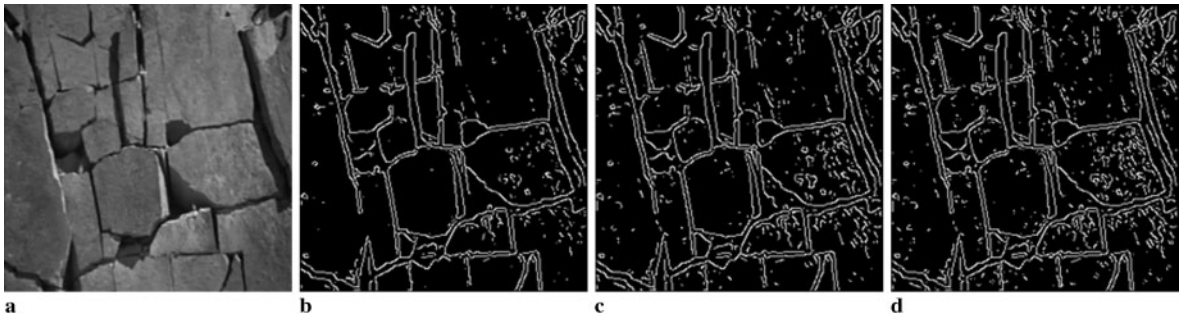

4 Experimental results of Rock fracture image: (a) original image; (b) result of traditional Canny; (c) result of reference;[17] (d) result of the new algorithm this paper

by applying the double-thresholds that are obtained by using maximum information cross-entropy between classes, and finally traces the object boundaries by a procedure for object closing if it needs.

The algorithm procedure can be briefly illustrated in the following eight steps.

Formal algorithm procedure description (not including object boundary closing):

1. Input an original grey-level image $f(x,y)$.
2. Smooth $f(x,y)$ twice by using the adaptive filter, obtain smoothed image $s(x,y)$.
3. Calculate directional derivatives and amplitudes for all the pixels in the image $s(x, y)$, then, got directional derivative matrices $D_x(x,y)$ and $D_y(x,y)$, and gradient magnitude matrix (image) $M(x,y)$.
4. Operate $D_x(x,y)$, $D_y(x,y)$ and $M(x,y)$ with non-maximum suppression.
5. Find out high threshold T_h and low threshold T_l by using the algorithm of maximum cross-entropy between classes and Bayesian judgment.
6. Search for edge points on the image $M(x,y)$ by using the thresholds T_h and T_l;
7. Output edge image $g(x,y)$.

In particle (multiple objects) images or particle-like images, the final result is to close all the object boundaries in the segmenting image. At this stage, in order to trace the boundaries of objects, the gaps between edges need to link. This task requires the extraction of information about attributes of endpoints of edges, in particular orientation and neighbourhood relationships.

As normal, after the above edge detection, the edges are thinned into a width of 1 pixel, but some gaps in the edges prevail and noise is still present in the image. To make closure of the object contours, it is necessary to trace edges (boundaries of objects). To do this, the procedure first detects significant endpoints of curves (or lines). Then, it estimates the directions for each endpoint based on the local directions of the edge pixels. Finally, it traces boundaries according to the information of directions of each new detected pixel (new endpoint) and an intensity cost function. The edge tracing starts from the detected endpoints to see which neighbourhood has the highest grey value, and when a new pixel is found as edge point, it is used as new endpoint. If the endpoint cannot be found, the threshold values are changed until a new endpoint is determined.

5 Experimental results on Lion image: (a) original image; (b) result of Canny; (c) result of reference;[17] (d) result of the new algorithm in this paper

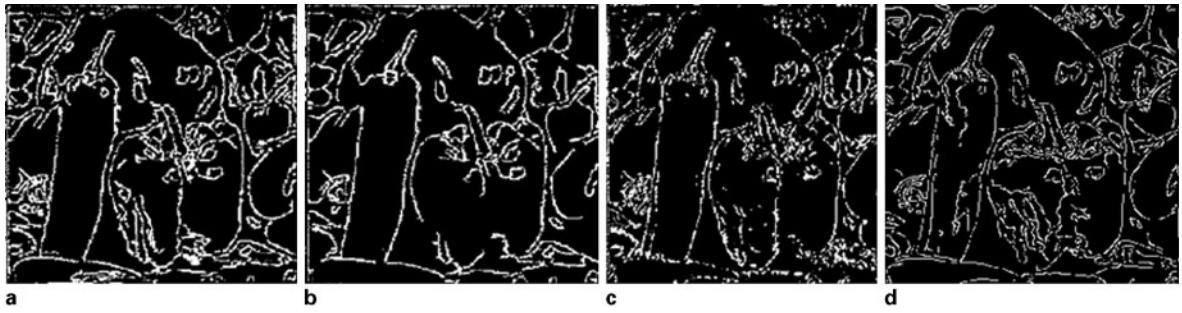

6 Experimental results of Pepper image in Fig. 3a: (a) result of proportion coefficient of threshold (0.4, 0.7); (b) result of proportion coefficient of threshold (0.5, 0.8); (c) result of reference;[7] (d) result of the new algorithm in this paper

Before it starts to trace from another detected endpoint, the tracing procedure continues until an object boundary is fully closed. When there is no detected endpoint for continuous tracing, the edge tracing procedure stops.

5 EXPERIMENTS

Experimental environment is that the operating system is Windows XP (SP3); the development platform is Visual Studio C++ 6.0, the computer RAM is 1024 MB and the frequency of CPU is 1.86 GHz. The algorithm testing and evaluation are carried out both subjectively and objectively respectively.

For the subjective evaluation, the four typical images were selected for presenting in this study, they are (1) Lena image; (2) Peppers image; (3) Fracture image; and (4) Lion image, where (1) and (2) are standard test images in the world, (3) has clear lines and curves and (4) has a huge number of thin edges.

From Fig. 2, one can see that markers 1–6 in Fig. 2b are not closed, markers 3 and 5 should have double edges; and markers 1, 2, 4 and 6 in Fig. 2c make closure better than those in Fig. 2b, but markers 1 and 2 in Fig. 2c are lost. All of the markers above are improved in Fig. 2d, where the results of the new algorithm in this study are presented.

It is clear from Fig. 3 that Pepper edges are not closed in Fig. 3b by using the tradition Canny algorithm, but the edge information is well detected in Fig. 3c; one can see from the original pepper image that there is much dark stripe information at the body of the peppers that are not detected by using the traditional Canny algorithm and the algorithm in Ref. 17. A satisfactory result is obtained by using the new algorithm studied in this paper.

In Fig. 4, the original image is a grey-scale image of rock fracture (Fig. 4a). Some fracture edges are of different widths and grey levels by using the traditional Canny algorithm. Though most of the fracture edges are detected in Fig. 4c by using the algorithm in reference,[17] some rock fracture burrs are obviously. By comparing Fig. 4b–c, the edge detection result is very well and rock fracture burr is greatly reduced in Fig. 4d when the new algorithm in this study is applied.

In Fig. 5, The most surface part of the image is rough exceptional to the four corners and the lion mouth. There are less edges on the both left and right sides of the lion head in Fig. 5b. More edges are detected in Fig. 5c than in Fig. 5b, but there still miss some edges compared to Fig. 5d. In Fig. 5d, most of the edges are detected except for the right side surface

Table 1 Experimental data of three algorithms

Image	Algorithm in Ref. 17			New algorithm in this study			Traditional Canny algorithm		
Name	Pixels (P)	Edges (E)	E/P %	Pixels (P)	Edges (E)	E/P (%)	Pixels (P)	Edges (E)	E/P (%)
Lena	9490	166	1.74	9498	151	1.59	6099	123	2.02
Peppers	9215	194	2.10	13 624	228	1.67	5457	169	3.10
Fracture	6580	424	6.44	7223	567	7.85	5416	295	5.45
Lion	6375	445	6.98	7183	560	7.79	5388	430	7.98

7 Experimental results of Lena image in Fig. 2a: (a) result of proportion coefficient of threshold (0.4, 0.7); (b) result of proportion coefficient of threshold (0.5, 0.8); (c) result of reference;[7] (d) result of the new algorithm in this paper

of the lion head, because the right side surface of the lion head is more flat than the other parts, and the smoothing filter will suppress the detailed information in the current resolution of images.

For the objective evaluation, there are a few points to discuss as the follows.

Wang[18] introduced an evaluation method for the effect of edge detection, where P represents the edge numbers detected and E represents the numbers of eight-connection in the edge image. The E/P reflects the degrees of linear edge connectivity, and the impact of edge linear connectivity for overall edge evaluation is reflected in wrong-detection and un-detection. When the edge connectivity is very poor, the numbers of wrong-detection and un-detection increase. In contrast, while the edge connectivity is higher, the numbers of wrong-detection and un-detection decrease. The smaller the values of the E/P, the better the degree of linear connectivity, and the better the edge effects extracted. The data in Table 1 show feasibility, superiority and robustness of the algorithm in this paper.

Li *et al.*[7] obtained double-thresholds by using gradient histogram and minimum interclass variance, and by comparison with different methods. Figures 6a and 7a are the results detected by using the traditional Canny algorithm, and proportional coefficient of high and low thresholds are (0.7, 0.4). To illustrate the fluctuations of proportional coefficient of high and low thresholds having some effects using the traditional operator, a set of proportional coefficients (0.8, 0.5) of high and low thresholds are particularly adopted when the experiments are carried out on the two images using the traditional Canny algorithm. Figures 6b and 7b are the test results. Figures 6c and 7c are the results from Ref. 7. Figures 6d and 7d are the results from this study. It is obvious from the contrast that the double-thresholds are different for the different images with the same proportional coefficient of high and low thresholds, such as in Figs. 6a and 7a, and the experiment results are different in the same image with different proportional coefficients of high and low thresholds, as shown in Figs. 6a and 7a. All of these illustrate that the proportional coefficient of high and low thresholds by artificial setting is obtained adaptively compared to a manual test method. Although it loses some details in Fig. 6a, the effect of overall detections is good; there are the satisfactory results in Fig. 7b, but having redundancy (noise) at the shoulder of the girl in the image which also shows that it is not scientifically using the same proportional coefficient for the different images, and it affects the detection result. Some detailed information in Fig. 6b and 7b is

8 Experimental results of Tiger image: (a) original grey-level image; (b) result of proportion coefficient of threshold (0.3, 0.9); (c) result of proportion coefficient of threshold (0.5, 0.6); (d) result of Ref. 7; (e) result of the new algorithm in this paper

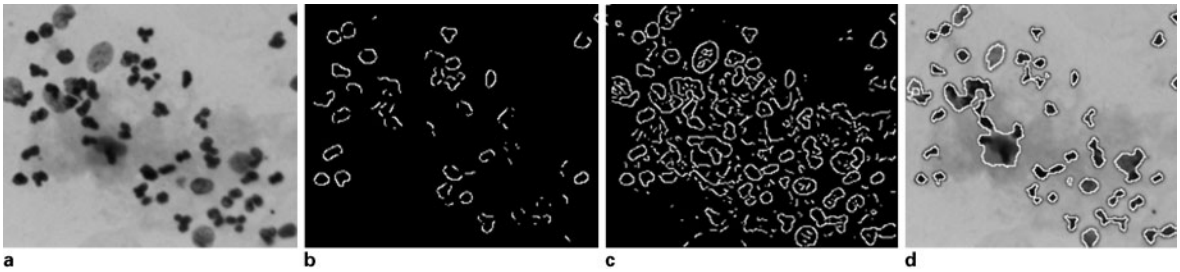

9 Experimental results of cell image: (a) original grey-level image; (b) result of proportion coefficient of threshold (0.3, 0.9); (c) result of the new algorithm in this paper; (d) cell closure result on (c)

lost. Figures 6c and d, and 7c and d show that though the double-thresholds are obtained adaptively and are not needed to set threshold artificially, this paper has a better result than that in reference.[7]

In the Canny edge detection algorithm, sometimes the high and low thresholds are very sensitive to the edge detection result. Figure 8 is one of the examples. The tiger head image includes much fine surface information; if the high threshold T_h is too high, only the edges of the black traps are detected, and the much fine surface information is missing as shown in Fig. 8b. When the T_h is set near to the low threshold T_l (e.g. 3–5) as shown in Fig. 8c, the variation of T_l is not sensitive to the detection result, and the result is closed to the result in Ref. 7. Anyhow, the edge detection by using the new algorithm presents the much more detailed and clear edge information than by using the other algorithms.

For the images including multiple particles with different sizes and shapes, it is usual that it needs to close all the particle boundaries. The boundary closing is mainly depending on the edge detection results when the image segmentation algorithm is discontinuous information based. Figure 9 shows a cell image (objects with different grey levels) and its processing results. It is difficult to close the cells on the image in Fig. 9b due to that some edges are missing. The similar situation is shown in Fig. 10, where the sizes and shapes of electronic particles need to measure. Figures 9 and 10 show that variable double-thresholds will affect object boundary closing more significantly, and the optimal threshold determination in this paper can greatly increase the right probability of object boundary closing.

6 CONCLUSION

When an image is smoothed by using Gaussian filter in the traditional Canny algorithm, some detailed information will be lost because Gaussian function has its own shortage and it leads to affect edge connectivity and edge closure. The proportion coefficient of the high and low thresholds needs to be artificially set up and has certain limitation, and cannot meet the requirements of adaptive adjustment for different images. This paper replaces original Gaussian function with an adaptive filter in different directions around the detecting pixel, in which way a suitable filter is chosen according to image properties

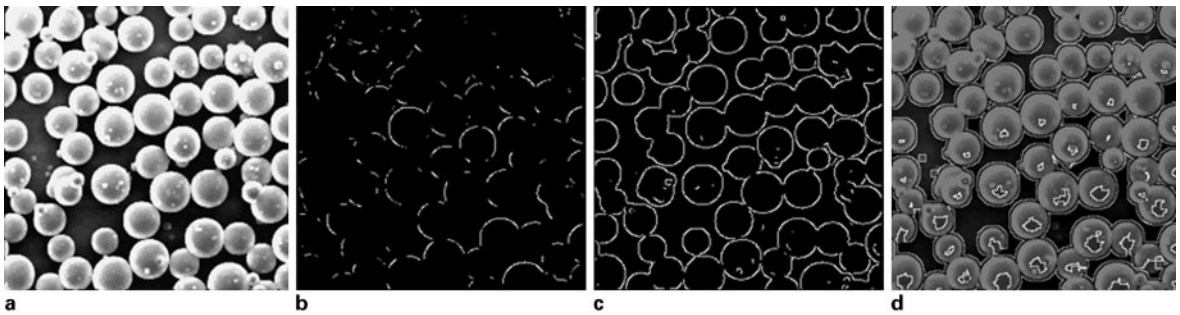

10 Experimental results of Particle image: (a) original grey-level image; (b) result of proportion coefficient of threshold (0.3, 0.9); (c) result of the new algorithm in this paper; (d) particle closure result on (c)

automatically. In the new algorithm, the double-thresholds for gradient magnitude images are obtained by combining the information of cross-entropy with Bayesian judgment theory. It is concluded from the analyses of the experimental results above that the modified algorithm has good adaptive characteristics. For the standard images (Figs. 2–4), the new algorithm performs better than the other algorithms as discussed above, and more edge details for the images including much fine surface information (Figs. 5, 8) can be abstracted in most of the cases. In addition to these, the object boundary closure is performed well for particle or particle-like images based on the studied edge detection algorithm (Figs. 9 and 10). Experiments show the good feasibility and robustness of the new algorithm in this study. The algorithm can be used in many applications.[18]

ACKNOWLEDGEMENTS

This work was supported in part by the New Century Excellent Talents plan projects (no. NCET-05-0849) and the National Natural Science Foundation (nos. 50978030 and 60873186).

REFERENCES

1 Shapiro, L. G. and Stockman G. C. Computer Vision, 2001, p. 326 (Prentice Hall, London).
2 Zhu, G. Y. and Zhang, R. L. Application of Canny operator on automatic detection of fabric waterproof performance. *J. Text. Res.*, 2008, **29**, 122–126.
3 Shao, X. F., Sun, J. X., Wang, L. L. and Tian, S. F. An improved Canny edge detection algorithm. *J. Electron. Opt. Control*, 2006, **13**, 53–55.
4 Wang, Y., Xiang, B. Q. and Huang, Y. Multidirection edge detection algorithm based on Canny theory. *J. Comput. Eng.*, 2007, **33**, 211–212.
5 Kaur, A. and Singh, R. Wavelets for edge detection in noisy images, Proc. Natl Conf. on *Computational instrumentation: NCCI 2010*, Chandigarh, India, March 2010, CSIO, pp. 184–186.
6 Bao, P., Zhang, L. and Wu, X. Canny edge detection enhancement by scale multiplication. *IEEE Trans. Patt. Anal. Mach. Intell.*, 2005, **27**, 1485–1490.
7 Li, M., Yan, J. H., Li, G. and Zhao, J. Self-adaptive Canny operator edge detection technique. *J. Harbin Eng. Univ.*, 2007, **9**, 1002–1007.
8 He, X., Jia, W. and Wu, Q. An approach of Canny edge detection with virtual hexagonal image structure, Proc. 10th Int. Conf. on *Control, automation, robotics and vision: ICARCV 2008*, Hanoi, Vietnam, December 2008, Nanyang Technological University of Singapore/ Vietnamese Academy of Science and Technology, pp. 879–882.
9 Ding, L. J. and Goshtasby, A. On the Canny edge detection. *Patt. Recogn.*, 2001, **34**, 721–725.
10 Lv, Z., Wang, F. L. and Chang, Y. Q. An improved Canny algorithm for edge detection. *J. Northeast. Univ. (Nat. Sci.)*, 2007, **28**, 1682–1685.
11 Li, W. B., He, M. Y. and Zhang, S. L. A new Canny-based edge detector for SAR image, Proc. 2008 Int. Cong. on *Image and signal processing: CISP2008*, Sanya, China, May 2008, IEEE Computer Society, pp. 211–215.
12 Rockett, P. I. and Zhang, Y. The Bayesian operating point of the canny edge detector. *IEEE Trans. Image Process.*, 2006, **15**, 3409–3416.
13 Chang, S. H., Gong, L. G., Li, M. Q., Hu, X. Y. and Yan, J. W. Small retinal vessel extraction using modified canny edge detection, Proc. 2008 IEEE Int. Conf. on *Audio, Languages, and Image Processing: ICALIP 2008*, Shanghai, China, July 2008, ICAD, pp. 1255–1259.
14 Canny, J. F. A computational approach to edge detection. *IEEE Trans. Patt. Anal. Mach. Intell.*, 1986, **8**, 679–698.
15 Sun, W., Xia, L. Z. and Pan, H. A new edge detection algorithm based on fuzzy partition. *J. Image Graph.*, 2004, **9**, 18–22.
16 Zhang, Y. J. Image Segmentation, 2005, pp. 120–121 (Tsinghua University Press, Beijing).
17 Wang, G.-Y. Study of Image Edge Detection Algorithm, 2008 (Chongqing University of Posts and Telecommunications, Chongqing).
18 Wang W. X. Fragment size estimation without image segmentation. *Imag. Sci. J.*, 2008, **56**, 91–96.